Structural and Magnetic properties of cadmium substituted Mg-Mn Ferrites Nanoparticles

Dr. K. R. Desai
Department Of Physics,
Balbhim Arts, Science and Commerce College
Beed, Maharashtra
M. S, India

ABSTRACT:

The sample of Mgx/2Mnx/2cd1-xFe2o4 spinel ferrite system with varying (x=0.0,0.2,0.4,0.6,0.8,1.0) Were Synthesized at temp 90c for 4h are investigated thoroughly synthesized by double sintering sol –gel method A.R grade oxides of magnesium, magnese, cadmium and ferric were used for the preparation of Mg Mn Cd fe2o4 ferrite all the synthesis powder were characterized by using X-ray diffraction(Philips x-ray diffracto-meter model 3710) The x-ray diffraction patterns were recorded in the 2 range of 20-80 using cu-kα radiation. The Magnetic properties were measured using provided by magenta company.

KEYWORDS: -Spinel Ferrite, sol-gel method, x ray diffraction, magnetic properties.

I. INTRODUCTION

Ferrite nanoparticles with spinal structure have attracted much attention due to their wide array of technological applicability in magnetic data storage gas sensors, magnetic resonance imaging magnetic drug delivery, energy storage etc.(1-3). In past few decades with the advent of nanotechnology .There has been renewe dinterest on synthesis of spinal ferrite nanoparticles with the potential application in the field of nanostructured materials spinel ferrites are widely used in many electronic device there are use in because of their high permeabilityin the radiofrquenency region high electrical resistivity mechanical hardness chemical stability and magnetic properties. (4-7)

It is known that the properties of Ferrites are depend on the various parameters that includes ,substitution of ions preparation of ionsapart from these reasons the properties of materials are also depending on the intrinsic strain induced 0n the lattice by these parameter. Ferrites are the magnetic properties are commonly used in electronic components.(8-11)

It is useful electrical magnetic properties used in magnetic fluid information storage and medical diagnostics (12-13) in recent years there has been considerable interest in the study of the properties of Nano sized ferrite particles because of their importance in the fundamental understanding of the physical properties as well as to their proposed application for many technological purposes. (14-15)

Types of nanoparticles can be produced by different wet chemical method such as co-precipitation(16)hydrothermal synthesis(17)Micro- emulsion synthesis(18)and sol-gel method(19)in addition various dry method including grinding (20)Mechanical alloying(21)and thermal plasma grinding (22)mechanical alloying(23)Thermal plasma methods(24)it is useful for ceramic method Properties of ferrites structural and magnetic strongly influenced by their composition prepration in this methodologies. In this work cdfe2o4 and Mgx/2Mnx/2cd1-xfe2o4 ferrite nanoparticles the structural refinement was done by using x-ray diffraction data. Elastic parameters were evaluated by using infrared spectra of the samples.

II .Materials and Methods

Sol-gel auto-ignition method was adopted to produce the nanoparticles of Mg2+-Mn2+ co-substituted cadmium ferrites having the general chemical formula Mgx/2Mnx/2Cd1-xFe2O4 (x = 0.0, 0.2, 0.4, 0.6,0.8, 1.0). All the starting chemicals with high purity (>99.5%) were purchased from Sigma-Aldrich and across which were used as received without any further purification. A. R. grade magnesium nitrate [Mg(NO3)2·6H2O], Ferric (III) nitrate [Fe(NO3)3·9H2O], manganese nitrate [Mn(NO3)2·6H2O], cadmium nitrate [Cd(NO3)2·6H2O] were dis-solved in sufficient amount of de-ionized water with their weight pro-portion. Citric acid was added in the mixture as a chelating agent in order to initiate the combustion process. The pH of whole mixture waskept constant at ≅7 by continuously pouring the liquid ammonia dropwise. The precursor was kept on magnetic stirrer with hot plate and the solution was

continuously stirred at a constant temperature of 90 °C.The continuous stirring with constant heating converts the solution into viscous gel by evaporating the excess solvents. The residual gel wasthen heated to 150 °C on hot plate forms the dried gel and after auto-ignition process it transforms into powder form. Final powders werecalcined at 800 °C for 6 h. Room temperature X-ray diffraction technique was adopted to confirm the crystal structure of the samples andto investigate the structural parameters. X-ray diffraction patterns ofall the samples were recorded on Ultima IV Rigaku X-ray diffracto-meter. The scanning range was taken from 2θ = 20°–80° with the scanning rate of 2°/min with Cu-Kα radiations (λ = 1.5405 Å). Infrared spectra of all the samples were recorded at room temperature in thewavenumber range of 300 cm−1to 800 cm−1 on Perkin Elmer.

III. Results and Discussion

Phase formation and crystal structure of Mgx/2Mnx/2Cd1-xFe2O4 ferrite nanoparticles have been investigated by using room temperature Xray diffraction (XRD). XRD patterns of all the samples were recorded in the 2θ range of 20°–80°. The main reflections were observed for the (220), (311), (400), (333), (440), (620) and (533) planes which are the characteristic peaks of cubic spinel structure. Some un-indexed peaks with very low intensity were observed for the samples x ≤ 0.6. These un-indexed peaks indicating that the secondary phase is present within the materials. To recognize the secondary phase, Rietveld refinement of all the samples was carried out by using full-proof software and the refined XRD patterns are shown in Fig. 3. Rietveld refinement confirmed that the sample x = 0.0, shows the cubic spinel structure and compatible with standard Card of CdFe2O4 (No. 96-591-0006) with space group of Fd-3m, while the sample x = 1.0 showed the single-phase cubic spinel structure and compatible with standard card of MgFe2O4 (No. 96-900-3600). The secondary phases of Fe2O3 (α-Fe2O3, No. 96- 210-8029, Space group R3c) and CdO (Space group Fm3m) were recognized for the samples x ≤ 0.8. The presence of these secondary phases could be the residue which remains un-reacted during the combustion process and sintering at lower temperature of 800 °C. The XRD patterns of CdFe2O4 containing Fe2O3 and CdO phases are also reported in literature [25–27]. Diffraction peaks of the host and doped samples showed minor shift in their positions towards higher diffraction angles which means that Mg2+ and Mn2+ ions were simultaneously replaced by the Cd2+ ions. These results are in accordance with the fact that the substituted ions accommodate the crystallographic sites [28]. Rietveld refinement of the XRD patterns was carried out by taking lattice constant, shape factors, scale factors as free parameters, the atomic fractional positions and occupancies as fixed parameters in account. Thompson-cox-Hasting pseudo-Voigt function was used to refine the background counts. The quantitative analysis of XRD patterns by Rietveld refinement can be related to the reliability factors viz. goodnessfactor (χ 2), R expected (RExp), profile factor (RP) and weighted profile factor (RWP). The ratio of RWP and RExp defines the χ 2 by through the relation [29]:

The x-ray (dx)percentage porosity(p) and specific surface area (s)were evaluated by using the relations discussed elsewhere(30,31)X-ray density dx shows decreasing trend while as porosity p and specific surface area s increases replacement of cd2+ions by Mg-Mn ions increases the specific area 'S'.Patterns of $Mg_{x/2}Mn_{x/2}CdFe_2O_4$ (A) x= 0.0, (B) x = 0.2, (C) x = 0.4, (D) x= 0.6, (E) x = 0.8 and (F) x = 1.0

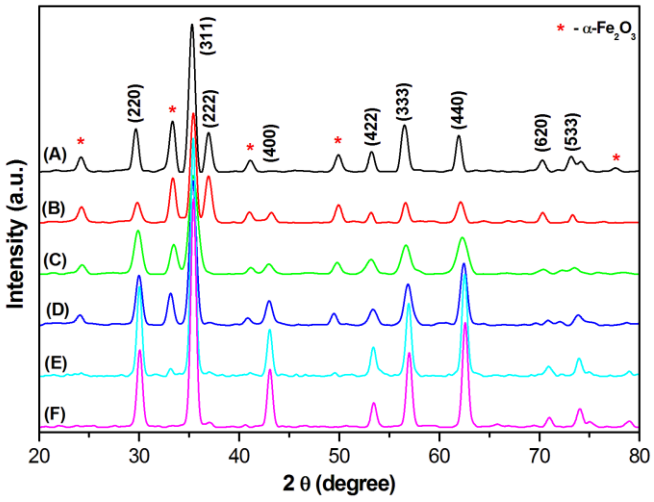

Fig:3.1

Table 3.1: Rietveld refined parameters, lattice constant (a), X-ray density (dx), porosity (P) and specific(s X-ray de surface area (s) of $Mg_{x/2}Mn_{x/2}CdFe_2O_4$

'x'	Rietveld Parameters	A (Å)	'd_x' (gm/cc)	P (%)	'S'			
	χ^2	R_{EXP} (%)	R_{WP} (%)	R_P (%)				
0.0	1.10	1.39	1.46	0.857	8.4587	6.324	39.72	60.90
0.2	1.246	1.369	1.529	1.111	8.4453	6.033	36.68	68.34
0.4	1.065	1.24	1.28	0.729	8.4301	5.743	32.84	76.38
0.6	1.292	1.509	1.716	1.236	8.4137	5.452	27.54	82.52
0.8	1.03	1.50	1.52	0.981	8.3976	5.156	25.84	92.10
1.0	1.01	1.01	1.02	0.468	8.3814	4.858	24.02	103.85

Scherrer method [30] is the most popular approach to estimate the crystallite size by using the broadening of Bragg's lines. Williamson – Hall method is [31] another approach which gives the better information of crystallite size and contributions of microstrains observed in the crystal lattice. Peak broadening is closely related to the crystallite size of the samples. As per literature review, peak broadening is produced may be due to the micro-strains in the crystal lattice alone or by combine effect of lattice strain and particle size [32,33]. One of the best approaches to consider the spectrum is strain and size induced peak broadening (β) as a function of 2θ [34]. The observed and instrumental broadening can be corrected by the following relations [35, 36];

$$B_{total}=\beta_{strain}+\beta_{size} \quad (1)$$

Table 3.2: Cation distribution and intensity ratio calculations of $Mg_{x/2}Mn_{x/2}CdFe_2O_4$

'x'	Cation Distribution		Intensity Ratios					
	A-Site	B-Site	I_{422}/I_{440}			I_{440}/I_{220}		
			Obs.	Cal.	R	Obs.	Cal.	R
0.0	$(Cd_{0.9}Fe_{0.1})$	$(Cd_{0.1}Fe_{1.9})$	0.5024	0.4955	0.0069	0.7540	0.7449	0.0091
0.2	$(Mg_{0.03}Mn_{0.07}Cd_{0.72}Fe_{0.18})$	$(Mg_{0.07}Mn_{0.03}Cd_{0.08}Fe_{1.82})$	0.4385	0.4474	0.0090	0.8266	0.8300	0.0034
0.4	$(Mg_{0.03}Mn_{0.14}Cd_{0.54}Fe_{0.29})$	$(Mg_{0.17}Mn_{0.06}Cd_{0.06}Fe_{1.71})$	0.4013	0.4018	0.0005	0.9072	0.9176	0.0105
0.6	$(Mg_{0.03}Mn_{0.21}Cd_{0.36}Fe_{0.40})$	$(Mg_{0.27}Mn_{0.09}Cd_{0.04}Fe_{1.60})$	0.3080	0.3446	0.0386	1.0365	1.0420	0.0055
0.8	$(Mg_{0.03}Mn_{0.28}Cd_{0.18}Fe_{0.51})$	$(Mg_{0.37}Mn_{0.12}Cd_{0.02}Fe_{1.49})$	0.2875	0.2932	0.0058	1.1961	1.2054	0.0093
1.0	$(Mg_{0.03}Mn_{0.35}Fe_{0.62})$	$(Mg_{0.47}Mn_{0.15}Fe_{1.38})$	0.2350	0.2355	0.0005	1.4477	1.4536	0.0058

The distribution of divalent and trivalent cations among octahedral and tetrahedral sites in the presently investigated samples were determined from the ratio of XRD lines /220/440 and /400. These planes are assumed to be sensitive to the cation distribution. the temperature and absorption factors are not taken into account in our calculations as they do not affect the intensity calculation. If

an agreement factor (R) is defined as in Eq. (2) the best-simulated structure which matches the actual structure of the sample will lead to a minimum value of R and the corresponding cation distribution is obtained for each hkl and h k l reflection pair considered,

$$R = \left| \left(\frac{I_{hkl}^{obs}}{I_{hkl}^{obs}}\right) - \left(\frac{I_{hkl}^{calc}}{I_{hkl}^{calc}}\right) \right| \quad (2)$$

The relative integrated in intensity (Ihkl) of a Bragg's line of XRD pattern was obtained through the relation [37];

$$I\ hkl - \backslash F\backslash^2 hkl P Lp \quad (3)$$

where, P is multiplicity factor, F is structure factor, LP is Lorentz polarization factor and is given by

$$Lp = \frac{1+Cos^2 2\theta}{Sin^2\theta\, Cos\theta} (4)$$

The atomic scattering factors and multiplicity factors can be found in the literature [11]. The obtained cation distribution by using the above equations is given in Table 3.2. Cd2+ and Mn2+ ions preferred the A-site with fractional amount towards B-site, whereasmost of the Mg2+ ions prefer B-site. The radius of A-site decrease while the radius of Bsite increases with the substitution of Mg-Mn ions due to the reduction of Cd2+ ions fromA-site and occupancy of Mg2+ ions at B-site which has comparatively high ionic radii thanthat of Fe2+ ions.

The theoretical lattice parameter 'ath' and oxygen positional parameter 'u' werecomputed through the relations

$$[38 ath = \frac{8}{3}\sqrt{3}\left[(r_a + R_o) + \sqrt{3}\,(r_\beta + R_o)\right] \quad (5)$$

$$U = [(r_a + R_o)\frac{1}{\sqrt{3a}} + \frac{1}{4}] \quad (6)$$

Where, rA, rB and RO are the radii of A-, B-sites and oxygen (1.32Å) respectively. Thevariation of 'ath' and 'u' with the increasing percentage of Mg-Mn ions is shown in Figure3.5 (b). In case of fcc cubic spinel structures; u lies near 0.375 Å where O2- ions areorganized approximately a cubic closed packing. However, in most of the cases such ideal value of u marginally distorted. In the present investigation, the value of u is higher than0.375 Å.

The various allied parameters; bond lengths (dAX and dBX), shared tetrahedral edge(dAXE), and shared and unshared octahedral edges (dBXE and dBXEU) were obtained through the relations[39]

$$d_a = a\sqrt{3}\,(u-1/4) \quad (7)$$

$$d_{\beta x}=a\,[3u^2-(11/4)u+43/64)]^{1'2} \quad (8)$$

$$d_{axe}=a\sqrt{2}\,(2u-1/2) \quad (9)$$

$$ad_{\beta xe}=\sqrt{2}(1-2u) \quad (10)$$

$$d_{\beta xeu}=a[4u^2-3u+(11/16)]^{1'2} \quad (11)$$

Variation of allied parameters with the substitution of Mg-Mn ions in CdFe2O4 is shown in Figure 3a. It can be observed that bond length of tetrahedral A-site reduces from 2.55Å to 1.988 Å while as octahedral bond length expands from 1.798 Å to 2.00 Å with the addition of Mg-Mn ions. dAXE decreased whereas dBXE and dBXEU increases with the substitution of Mg2+-Mn2+ for Cd2+ ions.

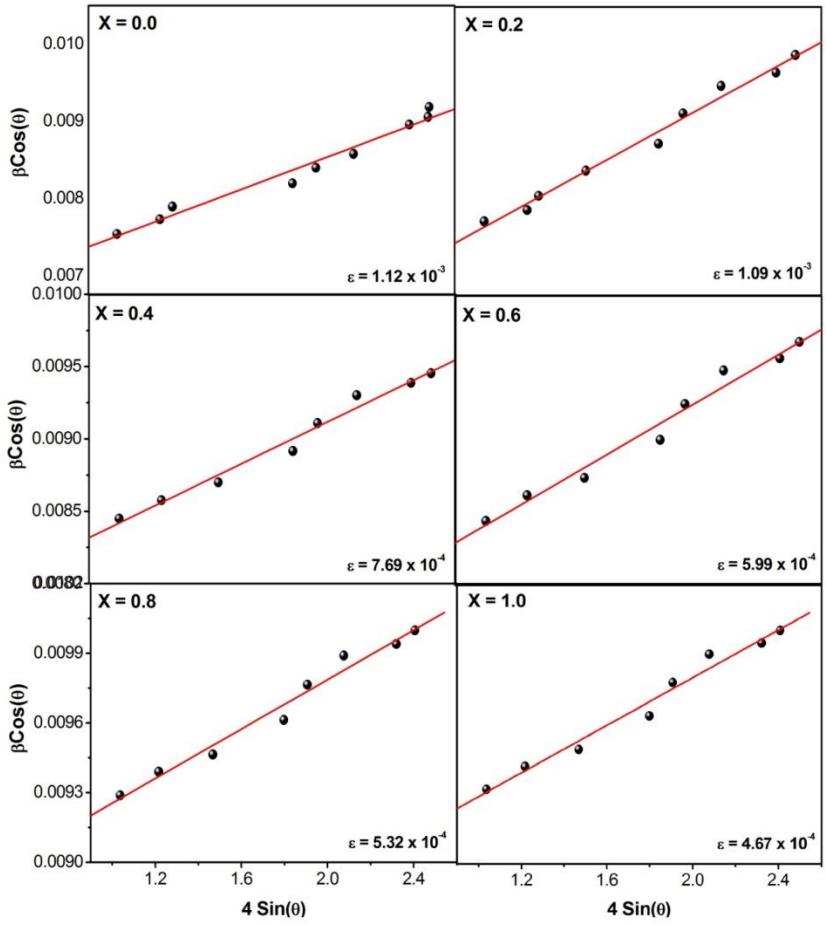

Fig.3: W-H PLOTS STRAIN ANALYSIS OF Mgx/2Mnx/2Cd1-xFe2O4

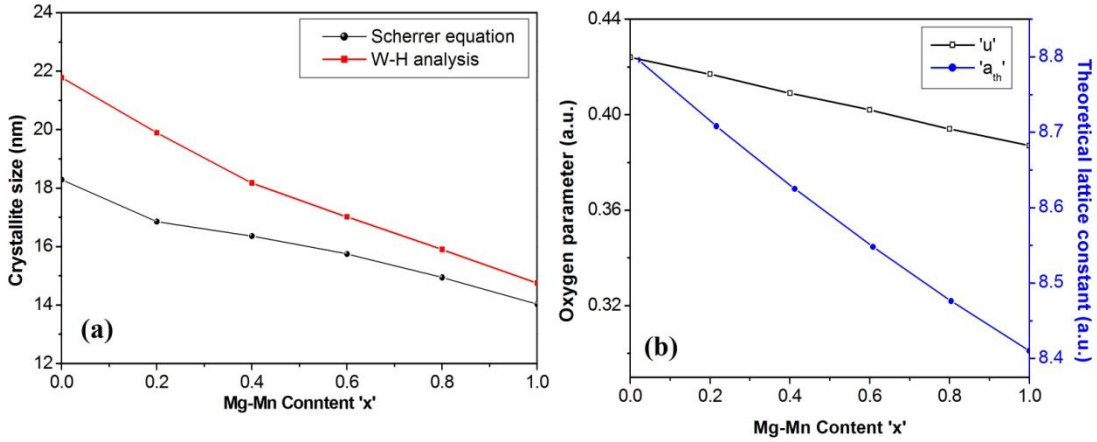

Fig. 3: (a) variation of crystallite size and (b) Oxygen positional par

ameter and theoretical lattice constant with Mg-Mn content 'x' for $Mg_{x/2}Mn_{x/2}CdFe_2O_4$

IV.CONCLUSIONS

Strain mechanism, cation distribution and elastic properties of Mg-Mnsubstituted Cd-ferrite nanoparticles by sol-gel auto-ignition method have been investigated in detail by W-H method, Bertaut method and infrared spectroscopy.the samples by using full-proof software and X-ray diffraction data confirmed the cubic spinel structure with the addition of secondary phase of α-Fe2O3 for the samples $x \leq 0.8$. The lattice parameter obtained from analysis shows decreasing trend from 8.4587 Å to 8.3814 Å with the substitution of Mg-Mn ions in CdFe2O4. The changes in lattice strain determined from W-H plots shows that all the samples possesses tensile type strain and it reduces with the addition of Mg-Mn ions. Cation distribution suggest that, Cd2+ and Mn2+ ions shows strong preference towards tetrahedral – A site while most of the Mg2+ ions prefers octahedral – B site. Stiffness constant and all the elastic moduli decrease with the replacement of Cd2+ ion by Mg2+-Mn2+ ions. Debye temperature decreases with the addition of Mg-Mn ions may be due to the dilution of P type conduction in the materials. The difference in the average ionic radii of Mg-Mn with that of Cd ions is the driving force to manipulate the properties of host CdFe2O4 spine ferrites.

REFERENCES

1. Z. Yan, J. Gao, Y. Li, M. Zhang, M. Guo; Hydrothermal synthesis and structureevolution of metal-doped magnesium ferrite from saprolite laterite; RSC. Advance; 5(2015) 92778.
2. M.A. Almessiere, Y. Slimani, S. Rehman, Firdos A. Khan, E. GökçePolat, A. Sadaqat, S. E. Shirsath, A. Baykal, Synthesis of Dy-Y co-substitutedmanganesezinc spinel Nano ferrites induced anti-bacterial and anti-cancer activities: Comparison between sonochemical and sol-gel auto-combustion methods, Mater. Sci. Engg. C 116 (2020) 111186.
3. E. F. Attia, A. H. Zaki, S. I. Deck, A. A. Farghali; Synthesis, physic chemicalproperties and photocatalytic activity of Nano sized Mg doped Mn ferrite; J. Mole. Liqu. 231 (2017) 589-596.
4. R. Peelamedu, C. Grimes, D. Agrawal, R. Roy, "Ultralow dielectric constant nickel–zinc ferrites using microwave sintering", J. Mater. Res., vol. 18, p. 2292, 2003.
5. A. K. M. AktherHossain, S. T. Mahmud, M. Seki, T. Kawai, H. Tabata, "Structural, electrical transport, and magnetic properties of $Ni_{1-x}\ Zn_x\ Fe_2\ O_4$", J. Magn. Magn.Mater. vol. 312, p. 210, 2007.
6. A. Goldman, Handbook of Modern Ferromagnetic Materials, KulwerAcademic Publishers, Boston, USA, 1999.
7. R. Valenzuela, Magnetic Ceramics, Cambridge University Press, Cambridge, 1994
8. S.E. Shirsath, D. Wang, S.S. Jadhav, M.L. Mane, S. Li, Ferrites obtained by sol-gelmethod, in: L. Klein, M. Aparicio, A. Jitianu (Eds.), Handbook of Sol-Gel Scienceand Technology, Springer, Cham, 2018, pp. 695-735.
9. A. S. Gaikwad, R. H. Kadam, S. E. Shirsath, S. R. Wadgane, J. Shah, R. K. Kotnala, A.B. Kadam, Surprisingly high magneto-electric coupling in cubic Co0.7Fe2.3O4-SrTiO3 nano-composites, J. Alloy. Compd. 773 (2019) 564-570
10. S.solyman Transport Properties of la-doped Mn-Zn ferrite ,ceramics International 32(2006)755-760
11. I.Sharifi ,H.shokrollahi ,S.Amiri ,ferrite –based magnetic Nano fluids used in hyperthermia applications Journal of magnetism and magnetic materials 324(2012)903-915
12. H.Shokrollahi journal of Magnetism and Magnetic Materials 320(2008)463-474
13. Influence of additives on Magnetic properties microstructure and densification of Mn-Zn soft ferrite materials science&engineeringB141(2007)91-107
14. Journal of magnetism &magnetic materials 288(2005)470-477
15. D.S Mathew R.S juang the structure &magnetism of spinel ferrite nanoparticles and their synthesis chemical Engineering journal 129(2007)51-65
16. J.L Darmann,D.Fiarani Magnetic properties of fine particles North Holland ,Amsterdam,1992.
17. Jonssan .p,Hanson M.F ,Nordbladp.phys.Rev .B2050,61,1261.
18. C.F Zhang ,X.C ZHONG Hy.Yu,Zw,Liu ,D,cZengphysicaB;condensed Matter 404(2009)2327-2331
19. Naibandian ,A.Delimitis ,V.T .Zaspallis ,E.aDellyanni D.N Bakooyannakis E.N,P eleka ,Micro porous materials 114(2008)465-473
20. P.P Hankare,R.P .PATIL ,U.B.Sankpal,S.D JADHAV,K.M GaradkarS.N,Achary,Journal of Alloys &compounds509(2011)276-280
21. B.Gillot ,B.DOMENICHINI,Materials Chemistry &physics 47(1997)217-224
22. S.Dasgupta,K.B Kim,J. Eckert,I. Manna,Journal of Aiioys&Compounds424(2006)13-20.
23. A.B Nawale,N.S ,Kanhe, J,Ellrich ,K.R Patil,S.V ,Bhoraskar,V.LMathe,A.K Das Journal of Alloys &compounds509(2011)4404-4413
24. A.CF.MCosta,E ,Tortella,M.RMorlli,R.H.G.AKiminami Journal of Magnetism &Magnetic Materials 256(2003)174-18
25. A .Banerjee, s.Bid,H.Dutta,s.Chaudhuri,D,Das,s.k pradhan,microstructure and positron annaihilation studies of mechanosynthesized cdfe2o4 J,Asain geram.soc 1(2013)356-361.
26. R.Ghasemi,J,Echeverria,J.I,Perezabal,J.J,Beat-Lopez,M.Naseri,C,Gomez-polo,Effect of cu substitution on the magnetic magnetic induction heating response of cdfe2o4 spinel ferrite,J,Magn matter,499(2020)166201.
27. M,Naseri,optical and magnetic properties of monophasic cadmium ferrite (cdfe2o4) nanostructure prepared by thermal treatment method,Jmagn mater.392(2015)107-117

28. K.Huang,j.Yu,l,Zhang,J,Xn,p,li,Z,Yang,c,Liu,W,Wang,X,Kan synthesis and characterization of magnesium and titanium doped M-type barium calcium hexaferrites by solid state recation method,J.alloys compd825(2020)154072
29. A.A Bagade,v.v Ganbavle,s.v Mohite,T,D,Dongle,b.b,sinha k,y Rajapure, Assessment of structural morphological,magnetic and gas sensing properties of cofe2o4 thin films,J,colloid Interface science497(2017)181-192
30. W. H. Hall, G. K. Williamson; Proc. Phys. Soc. 64B (1951) 937-946
31. . A. R. Stokes, A. J. Wilson, Proc. Phys. Soc. 65 (1944) 174
32. G. K. Williamson, W. H. Hall; X-ray line broadening from filled aluminum and wolfram; Acta. Mater. 01 (1953) 22-31.
33. T. Tatarchuk, M. Myslin, I. Mironyuk, M. Bououdina, A. T. Pedziwar, R. Gargula, B. F. Bogacz, P. Kurzydlo; Synthesis, morphology, crystallite size and absorption properties of nanostructured Mg-Zn ferrites with enhanced porous structure; J. Alloys. Comp. 819 (2020) 152945.
34. G. A. Kaur, M. Shandilya, P. Rana, S. Thakur, P. Uniyal, Modification of structural and magnetic properties of Co0.5Ni0.5Fe2O4 nanoparticles embedded polyvinylidene fluoride nanofiber membrane via electro-spinning method; Nano-Stru. Nano-Opjc. 22 (2020) 100428.
35. M. Kuru, T. S. Kuru, E. Karaca, S. Bagci; Dielectric, magnetic and humidity properties of Mg-Zn-Cr ferrites; J. Alloys. Comp. 836 (2020) 155318.
36. H. Kaur, A. Singh, V. Kumar, D. S. Ahlawat; Structural, thermal and magnetic investigations of cobalt ferrite doped with Zn2+ and Cd2+ synthesized by auto combustion method; J. Magn. Magn. Mater. 474 (2019) 505-511.

. 37 M.G. Buerger, Crystal Structure Analysis, Wiley, New York, 1960.
38 S. K. Gurav, S. E. Shirsath, R. H. Kadam, D. R. Mane; Low temperature synthesis of Li0.5ZrxCoxFe2.5-2xO4 powder and their characterizations; Powder technology, 235 (2013) 485-492

39 R. H. Kadam, A. R. Biradar, M. L. Mane, S. E. Shirsath; Sol-gel auto-combustion synthesis of Li3xMnFe2-xO4 and their characterizations; J. Appl. Phys. 112 (2012) 043902.